

Supplemental Information for Phonon thermodynamics and elastic behavior of GaAs at high temperatures and pressures

Jane E. Herriman^{1,2} and Brent Fultz¹

¹*Department of Applied Physics and Materials Science,
California Institute of Technology, Pasadena, California 91125, USA*

²*Quantum Simulations Group, Lawrence Livermore National Laboratory, Livermore, California 94550, USA*

I. LITERATURE COMPARISONS

In Table I we summarize elastic constant results from a few experimental (for zGaAs) and theoretical (for wGaAs and zGaAs) sources⁶⁻⁹, comparing these values to our own at 0K and 0 GPa. From Table I we see that our values for the elastic constants are much closer to experimental values^{7,9} than are e.g. values from the Materials Project⁶. Cui et. al⁸ seem to approach experimental values for zGaAs more closely than does the Materials Project, and our data for both zGaAs and wGaAs are much closer to data from Cui et al. than that of the Materials Project, increasing our confidence in our wGaAs data, given an absence of experimental values.

While the thermal expansion varies as a function of temperature, the linear coefficient of thermal expansion is reported as $5.73 \times 10^{-6} K^{-1}$ by ambient temperature⁴. Per our phonon calculations, we obtained an average linear coefficient of thermal expansion for zGaAs of $5.93 \times 10^{-6} K^{-1}$ between 0K and 1200K and of $4.60 \times 10^{-6} K^{-1}$ between 0 K and 600 K. For the same temperature ranges in wGaAs, we obtained average linear coefficients of thermal expansion of $5.31 \times 10^{-6} K^{-1}$ and $4.63 \times 10^{-6} K^{-1}$, respectively, but data are unavailable for this nonequilibrium material.

II. ADDITIONAL COMPUTATIONAL DETAILS

We evaluated a few potentials – AM05, LDA, and PBE GGA – and chose LDA because it performed the best according to metrics such as agreement with an experimental bulk modulus.

This work used standard projector augmented-wave (PAW) potential, without semi core states.

Zinc blende supercells were cubic with a uniform 0 K, 0 GPa lattice parameter of 16.8999 Angstroms. Wurtzite supercells were constructed to be as close to cubic as possible for the number of atoms used. At 0 K and 0 GPa, lattice vectors are expressed in Angstroms (as rows) as

$$\begin{pmatrix} 15.8769 & 0.0 & 0.0 \\ -7.9384 & 13.7498 & 0.0 \\ 0.0 & 0.0 & 19.6351 \end{pmatrix}$$

We used an adaptive Gaussian integration method implemented in TDEP to calculate phonon DOS. We used

$22 \times 22 \times 22$ brillouin-zone sampling meshes to generate phonon DOS and $14 \times 14 \times 14$ meshes to calculate phonon lifetimes.

Force constants were deemed converged when the phonon spectra converged. Convergence for phonon spectra was achieved when the amount of change between spectra was not impacted by the addition of further statistics and was deemed to be only noise; max noise for phonon spectra at each pressure and temperature point was around 1 meV or less.

III. ELASTIC ANISOTROPY

In Fig. 1 the universal elastic anisotropy index¹, A^U , derived from elastic constants, is shown as a function of pressure in wGaAs (purple) and zGaAs (blue). As in Figs. ?? and ?? of the main paper, a dashed line spanning the region between 15 and 20 GPa for wGaAs is a guide to the eye where real data has been omitted for the purpose of decoupling elastic constant calculations from the onset of a shorter wavelength phonon instability. A^U quantifies elastic anisotropy via

$$A^U = 5 \frac{G_V}{G_R} + \frac{K_V}{K_R} - 6, \quad (1)$$

where K and G are the bulk and shear moduli, and subscripts R and V denote Reuss and Voigt bounds on these quantities, respectively. While Reuss places lower limits on these quantities by assuming uniform stress, Voigt defines upper bounds on these quantities by assuming the material is under constant strain². In a perfectly elastically isotropic crystal, Reuss and Voigt bounds are equivalent and A^U is 0. Unlike more commonly used metrics for quantifying elastic anisotropy like the Zener ratio, A^U is independent of crystal structure.

Figure 1 shows that elastic anisotropy increases with pressure in both wGaAs and zGaAs. On the left we see that zGaAs is more elastically anisotropic at low pressures but wGaAs becomes more elastically anisotropic at 30 GPa. Elastic anisotropy increases with pressure exponentially in wGaAs. The graph at right shows how A^U for wGaAs far exceeds the anisotropy of zGaAs with increasing pressure.

Prior to the onset of instability, Fig. 1 shows that zGaAs is more elastically anisotropic than wGaAs. This is unlike the trend seen in GaN, where the wurtzite form,

		Theoretical			Experimental	
	Conditions	0 K, 0 GPa (this work) ³	0 K, 0 GPa ⁶	0 K, 0 GPa ⁸	extrapolated to 0 K, 0 GPa ⁹	298 K, 0 GPa ⁷
wGaAs	C_{11}	140	118	136	N/A	
	C_{12}	50	35	36		
	C_{13}	34	24	24		
	C_{33}	163	138	156		
	C_{44}	36	33	36		
zGaAs	C_{11}	116	99	112	123	118
	C_{12}	55	41	47	57	54
	C_{44}	57	51	60	60	59

TABLE I: Elastic constant data from this work at 0 K and 0 GPa, compared with a few literatures sources.

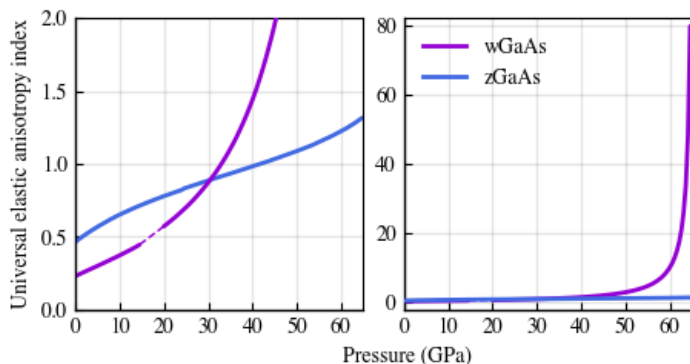


FIG. 1: Values for the universal elastic anisotropy index versus pressure for wGaAs in purple and zGaAs in blue. Elastic anisotropy increases with pressure for both materials, with zGaAs exhibiting greater elastic anisotropy than wGaAs in the regime where both phases are metastable. The dashed line in purple from 15 to 20 GPa spans the region of omitted data for C_{11} and C_{12} , as shown in Fig. ?? of the main text.

wGaN, was more elastically anisotropic than the zinc blende form, zGaN. Like the wurtzite and zinc blende forms of GaN, wGaAs and zGaAs become less elastically isotropic with increasing pressure. Nevertheless, we found wGaAs and zGaAs to be much less elastically anisotropic than GaN; even by the upper bound of lattice stability in wGaAs and zGaAs, the values for A^U in GaAs are approximately an order-of-magnitude smaller than those in GaN at 0 GPa³.

IV. PURELY TEMPERATURE-DRIVEN ANHARMONICITY

Figure 2 presents phonon dispersion relations for wGaAs and zGaAs at 0 and 1200 K, showing the effect of temperature on phonon frequencies; in each panel, differences between the blue and magenta curves indicate temperature-driven phonon frequency shifts. Across high symmetry directions, all phonon branches soften or do not change with temperature. In particular, the phonon

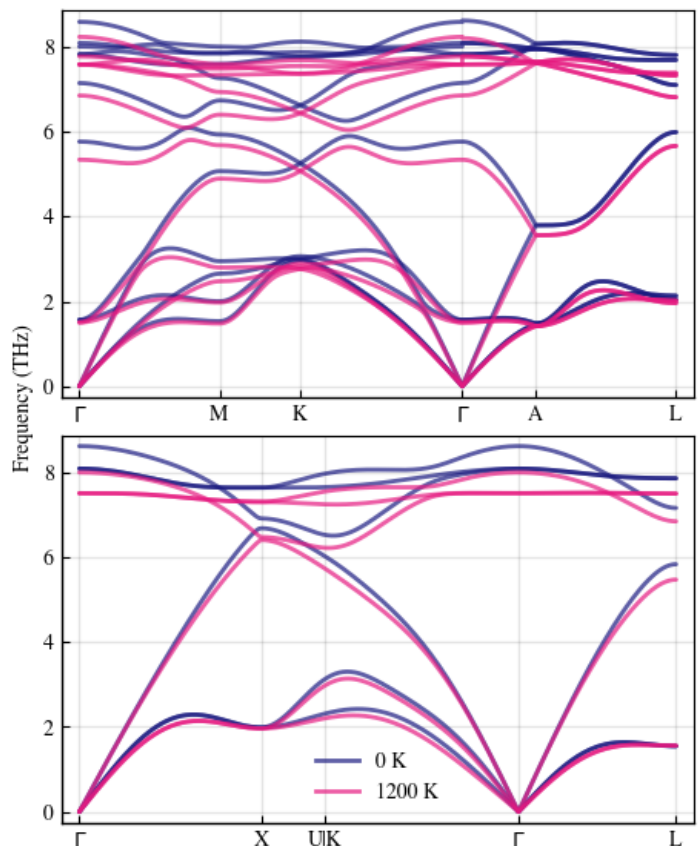


FIG. 2: Effect of temperature on the phonon dispersion relations of wGaAs (top) and zGaAs (bottom) at 0.0 GPa. For all phonon modes, temperature either has no effect, or induces softening, as the red curves are at lower frequencies than the purple curves.

modes that drive instability in each material do not seem to change with temperature between 0 and 1200 K.

V. PRESSURE-INDUCED FREQUENCY SHIFTS

Figure 3 compares the effects of pressure on phonon spectra of both wGaAs and zGaAs. All panels show overlays of 0 K phonon spectra at pressures of 0.0, 5.0, and 10.0 GPa. Panels (a) and (c) show phonon densities of states (DOS) for wGaAs and zGaAs, respectively, while (b) and (d) show phonon dispersions. Panels (a) and (c) show that higher frequency phonon modes shift even higher with increasing pressure. In contrast, lower frequency modes (i.e., below 4 THz) shift to even lower frequencies with increasing pressure, indicating negative Grüneisen parameters for some phonon modes. Panels (b) and (d) show more about the pressure-induced frequency shifts of modes along high symmetry directions. In wGaAs, the strongest softening with pressure occurs for the transverse acoustic modes at the M point and the lowest frequency transverse optical modes at Γ , each around 2 THz. In zGaAs, the most notable pressure-induced softening occurs for transverse acoustic modes at X and L , near and just below 2 THz. From results discussed in the main text, we know that pressure will cause the phonon frequencies of these modes to decrease until they become imaginary at the onset of instability.

VI. ANHARMONIC CALCULATIONS OF PHONON DECAY CHANNELS

The momenta and frequencies of decay channels depicted in Fig. 10 of the main text are summarized in Table II. Because several decay channels are depicted for each source mode and destination modes are consequently shown to have ranges, the frequencies and coordinates listed in Table II correspond to an average of those ranges.

VII. NEGATIVE GRÜNEISEN PARAMETERS

Phonon modes that stiffen with increasing pressure, and thereby decreasing volume, have positive Grüneisen parameters; those that soften under the same conditions have negative Grüneisen parameters. Figure ?? shows that most phonons in wGaAs and zGaAs stiffen with increasing pressure, indicating positive Grüneisen mode parameters, and that transverse acoustic phonon branches along certain high symmetry directions have negative Grüneisen parameters. In most materials, the stiffening of phonon modes with decreasing volume is typical, and drives thermal expansion. After all, as temperature increases, it alters the free energy landscape of the material; if the equilibrium volume that minimized the free energy at T no longer minimizes the free energy at $T + \delta T$, the material changes its volume to increase entropy.

For a set of N 3D classical harmonic oscillators, the

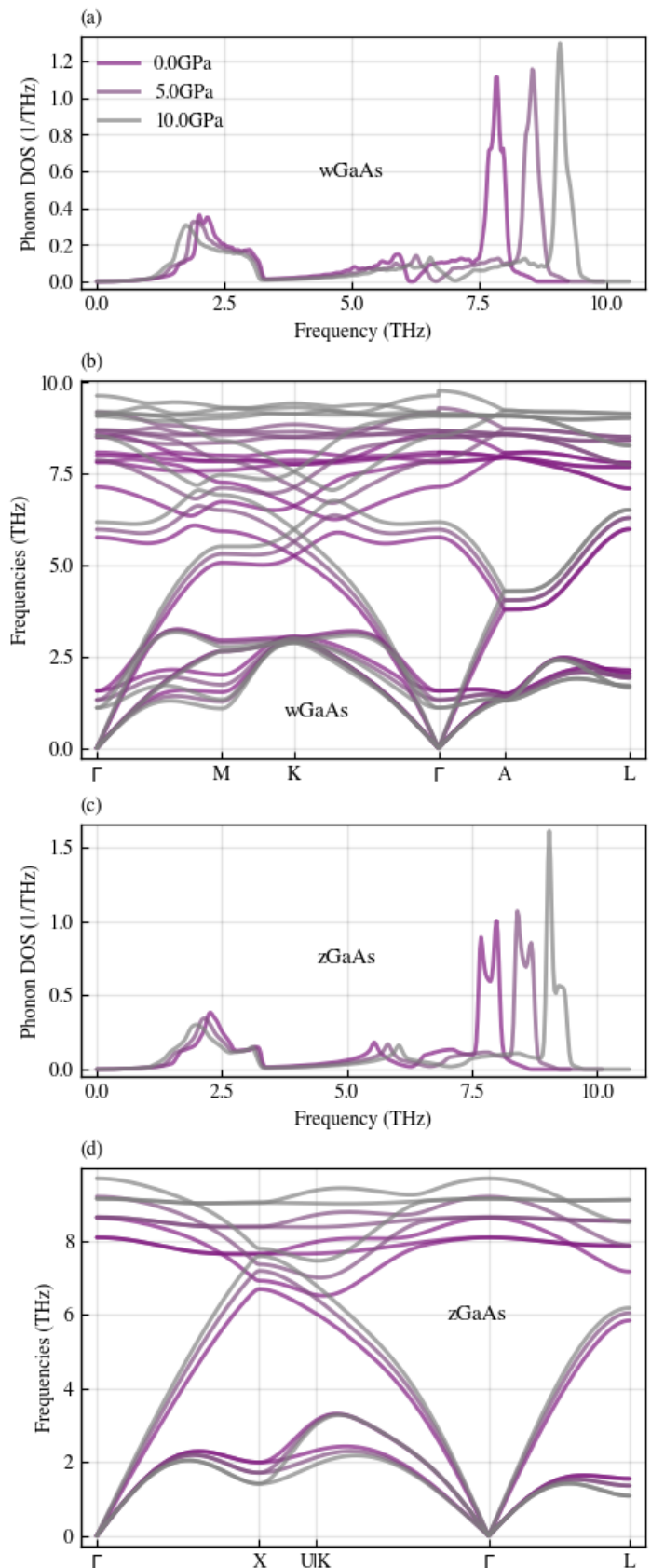


FIG. 3: Phonon DOS and dispersion relations at 0 K for three pressures for wGaAs ((a) and (b)) and zGaAs ((c) and (d)). Panels (c) and (d) show that the pressure-induced softening of the lower energy portions of the spectra from the transverse acoustic modes and, in (c), of one set of transverse optical modes. The most apparent softening occurs at the M and Γ points in wGaAs and at X and L in zGaAs.

material	pressure	q-coordinates			frequencies (THz)		
		source	dest 1	dest 2	source	dest 1	dest 2
wGaAs	0 GPa	0.436667 * [1, -0.5, 0]	0.111667 * [1, -0.5, 0]	0.325 * [1, -0.5, 0], 5.4 THz	6.1	0.7	5.4
	10 GPa	0.436667 * [1, -0.5, 0]	0.176667 * [1, -0.5, 0]	0.26 * [1, -0.5, 0]	6.9	1.0	5.9
	0 GPa	0.449749 * [1, 0, 0]	0.0728643 * [1, 0, 0]	0.376884 * [1, 0, 0]	6.3	0.5	5.8
	10 GPa	0.449749 * [1, 0, 0]	0.175879 * [1, 0, 0]	0.273869 * [1, 0, 0]	7.1	5.8	1.3
zGaAs	0 GPa	0.74625 * [0.5, 0.5, 1]	0.3375 * [0.5, 0.5, 1]	0.40875 * [0.5, 0.5, 1]	5.7	1.6	4.1
	10 GPa	0.74625 * [0.5, 0.5, 1]	0.136875 * [0.5, 0.5, 1]	0.609375 * [0.5, 0.5, 1]	6.6	0.7	5.9
	0 GPa	0.43 * [1, 1, 1]	0.04 * [1, 1, 1]	0.39 * [1, 1, 1]	5.3	0.3	5.0
	10 GPa	0.43 * [1, 1, 1]	0.0375 * [1, 1, 1]	0.3925 * [1, 1, 1]	5.8	0.3	5.6

TABLE II: This table summarizes the decay channels depicted in Fig. 10 of the main text. For each material and pressure, “destination” modes sum to “source” modes, conserving both energy (via additive frequencies) and crystal momenta (via additive q-coordinates).

vibrational entropy, S_{vib} , can be expressed cleanly as

$$S_{\text{vib}} = -\frac{\partial F_{\text{vib}}}{\partial T} = -k_B \ln \left(\prod_{i=1}^{3N} \frac{\hbar\omega_i}{k_B T} \right). \quad (2)$$

Because for $y = -\ln(x)$, y increases as x decreases, the vibrational entropy increases (and free energy decreases) when changes in volume reduce the phonon frequencies, $\{\omega_i\}$. If a phonon mode stiffens with increasing pressure, shifting to lower frequencies with increasing volume, it will help to drive (positive) thermal expansion. On the other hand, decreasing volume with increasing temperature lowers the vibrational energy contribution to the free energy of phonon modes with negative Grüneisen parameters. For this reason, negative Grüneisen parameters are often associated with negative thermal expansion (NTE), though NTE occurs only when the contributions to the free energy from those modes with negative Grüneisen parameters dominate the modes with positive Grüneisen parameters. Pressure-induced softening of transverse acoustic modes in GaAs is consistent with findings that zGaAs exhibits negative thermal expansion up to about 60 K.⁴ However, there may be a role for anharmonicity and the zero point atom displacements at low temperature, as was recently shown for silicon⁵.

VIII. COMPARISON WITH $P - T$ COUPLING EFFECTS IN GALLIUM NITRIDE

Figure ?? of the main text shows that in both wGaAs and zGaAs, the QHA less accurately accounts for thermal frequency shifts at high pressures. In GaAs, pressure seems to enhance the importance of explicitly anharmonic phonon effects in accounting for temperature-driven phonon behavior. Figure 4 is an analog to Fig. ?? of the main text, using GaN phonon data from our previous work³. In GaN, the effect of pressure on the reliability of the QHA is less important than in GaAs. Panel (b) shows that pressure slightly augments phonon stiffening around 20 THz caused by explicit temperature-driven

anharmonicity in wGaAs; on the other hand, effects of pressure on temperature-driven anharmonicity in zGaAs are hard to detect with panels (c) and (d). Our use of more extreme pressures in GaN than in GaAs makes it more likely that we would observe the $P - T$ coupling effects in GaN than in GaAs.

Instead of comparing $P - T$ coupling results in GaAs at 1200 K to GaN at 1120 K, it may be better to compare at temperatures scaled by their Debye temperatures. The Debye temperature of GaN (≈ 600 K) is about 1.67 times that of GaAs (≈ 360 K). Temperature effects in GaAs by 600 K may be a better comparison to those in GaN by 1120 K. In Fig. 5, we see that even at 600 K, the impact of pressure on temperature-driven anharmonicity in GaAs is clear, and much more evident than in Fig. 4. Although we observed other pressure-temperature coupling effects in both wGaAs and zGaAs³, pressure-temperature coupling in wGaAs and zGaAs seems more pronounced.

IX. ESTIMATING PHONON INSTABILITY ONSET FROM γ

The i^{th} mode Grüneisen parameter is defined as

$$\gamma_i = \frac{-V}{\omega_i} \frac{\partial \omega_i}{\partial V} \approx \frac{-V}{\omega_i} \frac{\Delta \omega_i}{\Delta V}. \quad (3)$$

We can use this equation to estimate the volume at which phonon instability occurs by calculating the volume change associated with a phonon frequency shift to 0 THz.

Assume that pressure “H” is the highest pressure for which we have stable data and that pressure “I” is the pressure at which the first phonon mode to become unstable softens to 0 THz. Call that first phonon “X” (as in the case of zGaAs). Its Grüneisen parameter is

$$\gamma_{X,H} \approx \frac{-V_H}{\omega_{X,H}} \frac{\omega_{X,I} - \omega_{X,H}}{V_I - V_H}. \quad (4)$$

Here, $\omega_{X,I}$ is 0 THz, the frequency at which the X mode first becomes unstable, and V_I is the associated volume.

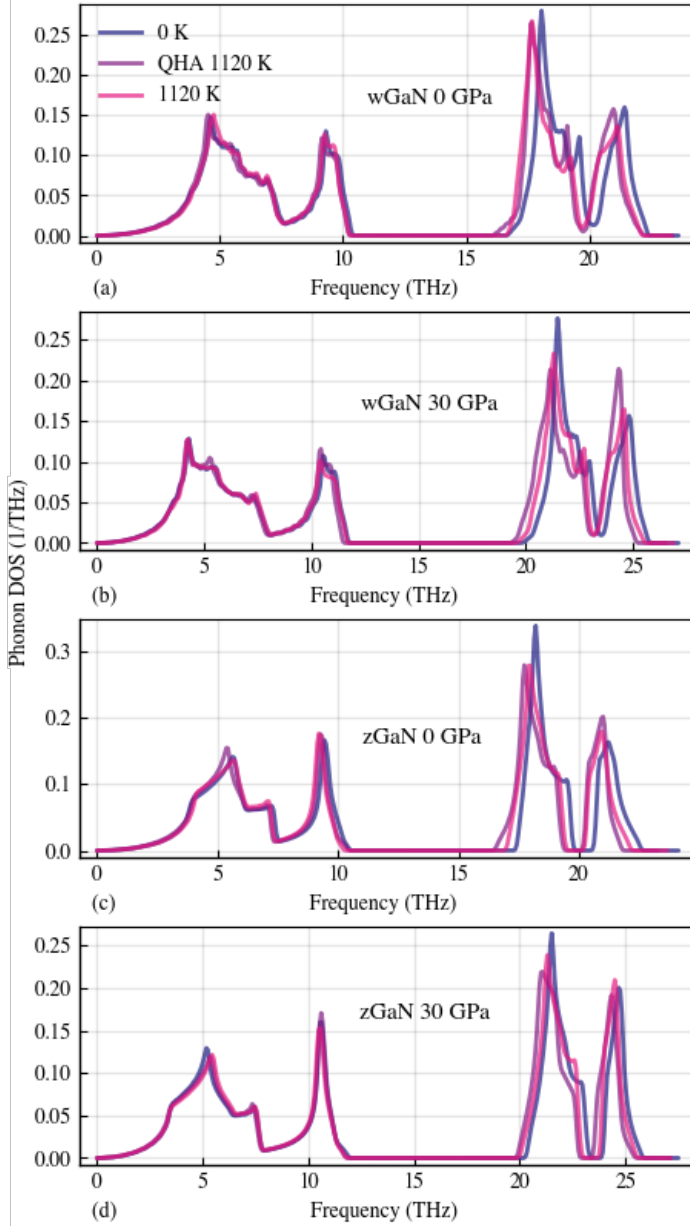


FIG. 4: Overlays of phonon DOS at 0 K and at 1120 K per a QHA and with full anharmonic phonon effects are shown at (a) 0.0 GPa in wGaN, (b) 30.0 GPa in wGaN, (c) 0.0 GPa in zGaN, and (d) 30.0 GPa in zGaN.

Similarly, $\omega_{X,H}$, V_H , and $\gamma_{X,H}$ are the frequency, volume, and Grüneisen parameter at X of the phonon branch to go unstable at the highest pressure for which we have data. Equation 3 becomes

$$\gamma_{X,H} \approx \frac{-V_H}{\omega_{X,H}} \frac{-\omega_{X,H}}{V_I - V_H} \approx \frac{V_H}{V_I - V_H}. \quad (5)$$

The volume of the onset of lattice instability is V_I

$$V_I \approx \frac{V_H}{\gamma_{X,H}} + V_H. \quad (6)$$

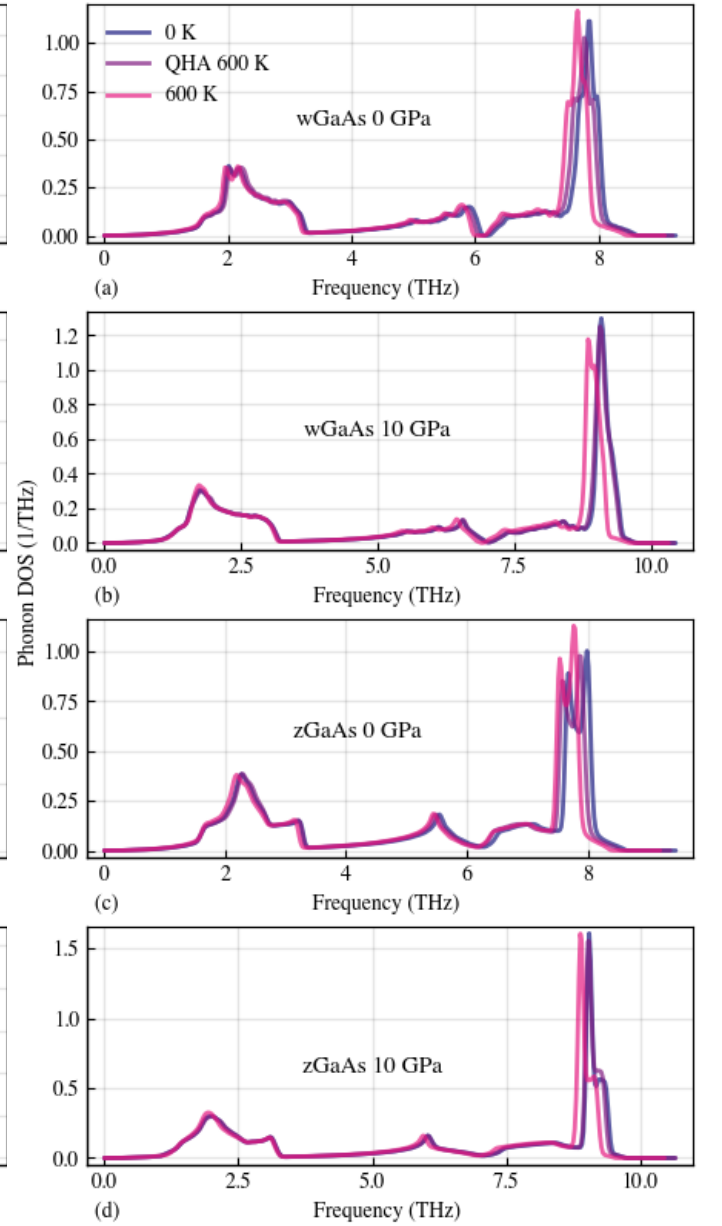


FIG. 5: Overlays of phonon DOS at 0 K and at 600 K per a QHA and with full anharmonic phonon effects are shown at (a) 0.0 GPa in wGaAs, (b) 10.0 GPa in wGaAs, (c) 0.0 GPa in zGaAs, and (d) 10.0 GPa in zGaAs.

With V_I , the associated pressure, P_I is found by fitting to a Birch-Murnaghan equation of state.

The two largest sources of error in using this approximation come from extrapolation of pressure-volume relations, and the inequality of $\gamma_{X,H}$ and $\gamma_{X,I}$. When we use $\gamma_{X,H}$ to approximate the volume change until instability, we assume that the Grüneisen parameter at X will not change with volume, though we know that it does. Our estimates for V_I should place lower bounds on V_I (upper bounds on P_I). We used phonon data to estimate the pressures of instability onset. These estimates are

approximate. Pressure-volume relationships come from a Birch-Murnaghan equation of state fitted to the sum of the 0K static total energy and the phonon free energies versus volume, and depends on accurate phonon free energies. Once the phonon dispersion relations show a clear instability, the corresponding phonon free energies cannot reliably be used to determine the pressure at

that volume; this means that we can calculate the pressures for volumes smaller than those for which we have obtained stable phonon data only by extrapolation. Extrapolating the free energy surface of each material to slightly smaller volumes than those for which we have stable phonon dispersion relations does allow a general understanding of material behavior.

-
- ¹ S. I. Ranganathan and M. Ostoja-Starzewski, *Phys. Rev. Lett.* **101**, 055504 (2008).
- ² R. Hill, *Proc. Phys. Soc. Section A* **65**, 349 (1952).
- ³ J. E. Herriman, O. Hellman, and B. Fultz, *Phys. Rev. B* **98**, 214105 (2018).
- ⁴ S. I. Novikova, *Sov. Phys. Solid State* **3**, 129 (1961).
- ⁵ D. S. Kim, O. Hellman, J. Herriman, H. L. Smith, J. Y. Y. Lin, N. Shulumba, J. L. Niedziela, C. W. Li, D. L. Abernathy, and B. Fultz, *Proc. Natl. Acad. Sci.* **115**, 1992 (2018).
- ⁶ A. Jain, S. P. Ong, G. Hautier, W. Chen, W. D. Richards, S. Dacek, S. Cholia, D. Gunter, D. Skinner, G. Ceder, et al., *APL Materials* **1**, 011002 (2013).
- ⁷ H. J. McSkimin, A. Jayaraman, and P. Andreatch, *Journal of Applied Physics* **38**, 2362 (1967).
- ⁸ H.-L. Cui, F. Luo, X.-R. Chen, and G.-F. Ji, *Canadian Journal of Physics* **87**, 153 (2009).
- ⁹ C. W. Garland and K. C. Park, *Journal of Applied Physics* **33**, 759 (1962).